

Structural characterization of lignin from *D. sinicus* by FTIR and NMR techniques

Zhengjun Shi, Gaofeng Xu, Jia Deng, Mengyao Dong, Vignesh Murugadoss, Chuntai Liu, Qian Shao, Shide Wu & Zhanhu Guo

To cite this article: Zhengjun Shi, Gaofeng Xu, Jia Deng, Mengyao Dong, Vignesh Murugadoss, Chuntai Liu, Qian Shao, Shide Wu & Zhanhu Guo (2019) Structural characterization of lignin from *D. sinicus* by FTIR and NMR techniques, Green Chemistry Letters and Reviews, 12:3, 235-243, DOI: [10.1080/17518253.2019.1627428](https://doi.org/10.1080/17518253.2019.1627428)

To link to this article: <https://doi.org/10.1080/17518253.2019.1627428>



© 2019 The Author(s). Published by Informa UK Limited, trading as Taylor & Francis Group



Published online: 18 Jun 2019.



Submit your article to this journal [↗](#)



Article views: 2143



View related articles [↗](#)



View Crossmark data [↗](#)



Citing articles: 56 View citing articles [↗](#)

Structural characterization of lignin from *D. sinicus* by FTIR and NMR techniques

Zhengjun Shi^{a,b}, Gaofeng Xu^{a,b}, Jia Deng^a, Mengyao Dong^c, Vignesh Murugadoss^c, Chuntai Liu^{c,d}, Qian Shao^e, Shide Wu^f and Zhanhu Guo^c

^aKey Laboratory for Forest Resources Conservation and Use in the Southwest Mountains of China, Ministry of Education, Southwest Forestry University, Kunming, People's Republic of China; ^bCollege of Chemical Engineering, Southwest Forestry University, Kunming, People's Republic of China; ^cIntegrated Composites Laboratory (ICL), Department of Chemical and Biomolecular Engineering, University of Tennessee, Knoxville, TN, USA; ^dKey Laboratory of Materials Processing and Mold (Zhengzhou University), Ministry of Education, National Engineering Research Center for Advanced Polymer Processing Technology, Zhengzhou University, Zhengzhou, People's Republic of China; ^eCollege of Chemical and Environmental Engineering, Shandong University of Science and Technology, Qingdao, People's Republic of China; ^fHenan Provincial Key Laboratory of Surface and Interface Science, Zhengzhou University of Light Industry, Zhengzhou, China

ABSTRACT

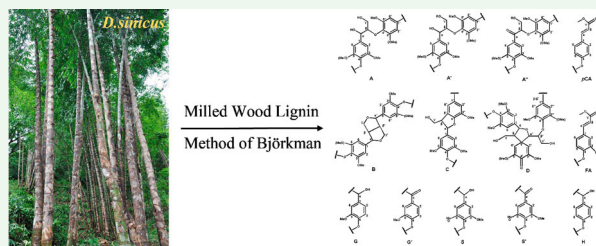
Milled wood lignin (MWL) was isolated from *Dendrocalamus sinicus*, an abundant bamboo variety in the earth, using Bjorkman method. Elucidation and quantification of the chemical structures for the isolated MWL have been facilitated by employing FT-IR and NMR techniques. The obtained results showed that the MWL consists of syringyl (S), guaiacyl (G), and *p*-hydroxyphenyl (H) units, indicating it as grass type (HGS) lignin. There is no significant change in structure (i.e. cleavage at α -O-4' and β -O-4' linkage) was observed. NMR techniques indicated that the isolated lignin was rich in β -O-4' aryl ether substructures and syringyl (S) units. Furthermore, the sufficient understanding of the chemical structure of the lignin benefits their effective utilization towards the production of renewable biomass and biofuels.

ARTICLE HISTORY

Received 22 September 2018
Accepted 31 May 2019

KEYWORDS

Bamboo; lignin; structural characterization; FT-IR; NMR





1. Introduction

Both depletion of fossil-based fuels and environmental issues have prompted the necessity to seek alternative renewable resources (1). Renewable biomass is one of the candidates based on forestry and several crops (2, 3). As an abundant bamboo species with fast-growing and high productivity, *Dendrocalamus sinicus* (*D. sinicus*) has become a mainly distributed hardwood species in the southwest of China (with the maximum diameter and height of 30 and 33 cm, respectively), which can be considered as potential resources for bio-refinery in China (4).

Lignin, a constituent of woody plant, is an ample aromatic biopolymer after cellulose and hemicelluloses. Lignin is primarily composed of following three phenylpropanoid units such as syringyl (S), guaiacyl (G), and *p*-

hydroxyphenyl (H), linked through ether and carbon-carbon bonds such as β -O-4', β - β' , α -O- γ' , γ -O- α' , β -1', 4-O-5', β -5, and 5-5' (5). In addition, lignin and hemicellulose are linked covalently by different chemical substructures such as benzyl-ether, phenyl glycosides, and benzyl-ester, forming lignin-carbohydrate complexes (LCC) (6). The knowledge of the chemical structure of lignin helps us to understand the separation and pretreatment mechanisms as well as to assess the potential exploitation of lignin for various applications (7). Physicochemical characteristics of the alkaline aqueous solution with soluble lignin of this special bamboo species have been reported (8). The obtained results indicated that the lignin interlinkages were cleaved to a certain degree under the alkaline conditions. *D. sinicus* is one of the abundant and

CONTACT Jia Deng  dengjia1983@163.com; Zhanhu Guo  zgou10@utk.edu

© 2019 The Author(s). Published by Informa UK Limited, trading as Taylor & Francis Group
This is an Open Access article distributed under the terms of the Creative Commons Attribution License (<http://creativecommons.org/licenses/by/4.0/>), which permits unrestricted use, distribution, and reproduction in any medium, provided the original work is properly cited.

potential renewable feedstocks for bio-energy, biofuel and lignocellulosic biorefinery (9). However, the presence of lignin-carbohydrate complexes (LCC) hampers the effective isolation of the wood constituents and the efficacy of enzymatic hydrolysis of carbohydrates in the biorefining process. Therefore, it is necessary to understanding the specific structural characteristics of lignin to develop an efficient and economical conversion technology for lignocellulosic resource biorefinery, which not clearly elucidated yet.

For an in-depth structural characterization of lignin polymer present in the bamboo species, the milled wood lignin (MWL) of bamboo (*D. sinicus*) was isolated under a mild condition according to the recognized method of Björkman (10). The structural characteristics of the isolated bamboo lignin were investigated by Fourier transform infrared (FT-IR) and nuclear magnetic resonance (^{13}C NMR and HSQC NMR) spectroscopy in detail.

2. Material and methods

2.1. Materials

Bamboo wood was collected from the three-year-old tree of *D. sinicus* harvested from Yunnan Province, China. The collected raw material was air-dried under the sun and then ground into sawdust using 40–60 mesh fraction. The dewaxed wood obtained after the extraction with ethanol/toluene (1:2, v/v) in a Soxhlet apparatus for 6 h were further dried at 60°C for 16 h. According to the technical report of National Renewable Energy Laboratory's (NREL), the lignin accounted for 28.57% of the total composition of these extract of *D. sinicus* on a dry weight basis (11). Finally, the dewaxed wood was ball-milled as reported in the earlier literature (12). All the other chemicals were procured from Sigma Chemical Company (Beijing, China).

2.2. Isolation of lignin fraction

The milled wood lignin (MWL) was isolated from bamboo (*D. sinicus*) by Bjorkman method with the following procedure; The treatment was carried out by suspending the ball-milled powder of dewaxed wood in 96% dioxane at a ratio of 1:20 (g/mL) at room temperature in dark for 24 h under the nitrogen atmosphere. After the incubation, the residual solid separated from the above mixture by filtration was washed sufficiently with the solvents, and lignin was precipitated as reported by Sun et al. (13). Firstly, the pH of obtained filtrates was neutralized to 5.5 using 6M HCl under reduced pressure in the rotary evaporator. Hemicellulose was then obtained by adding the neutralized

filtrate to 95% ethanol. The obtained hemicellulose was washed with 70% ethanol, and the resultant filtrate was freeze-dried. Thereafter, the pH of the concentrated filtrate was adjusted to 1.5–2.0 using 6M HCl to isolate 96% dioxane soluble lignin.

2.3. Characterizations of lignin fraction

The dried samples of isolated MWL was mixed with BaF_2 and then ground and pelletized to record their FT-IR spectrum. FTIR spectrum was recorded from 700 cm^{-1} to 4000 cm^{-1} at the resolution of 4 cm^{-1} using the iN10 FT-IR Microscope (Thermo Nicolet Corporation, Madison, WI, USA).

The solution-state ^{13}C -NMR and two-dimensional heteronuclear single quantum coherence (2D – HSQC) spectroscopy were recorded using the solution containing 80 mg of isolated MWL in 0.5 mL dimethyl sulfoxide- d_6 (DMSO, 99.8%) on Bruker AV III 400 MHz NMR spectrometer. The ^{13}C -NMR spectrum was recorded after 30,000 scans at 25°C. The 2D HSQC spectrum was recorded in the HSQC GE experiment mode. The spectral widths were 5000 for the ^1H - dimensions and 20,000 Hz for the ^{13}C -dimensions. 1024 complex points were collected with recycle delay of five seconds for the ^1H - dimension. The number of transients was 128, and 256-time increments in the ^{13}C -dimension. The 146 Hz of $^1\text{J}_{\text{C-H}}$ was used. In the ^{13}C -dimension, data matrix was zero filled up to 1024 points before Fourier transform. The standard Bruker Topspin-NMR software was used for data processing.

3. Results and discussion

3.1. FT-IR spectrum

The FT-IR spectrum of the lignin fraction isolated from the *D. sinicus* is shown in Figure 1. According to the previously reported data (14, 15), the absorption bands in the spectrum were associated with the characteristic functional groups of lignin. The broad absorption band at 3427 cm^{-1} was attributed to the -OH stretching vibration, while the band at 2940 cm^{-1} is assigned to the C–H symmetrical vibration of the methylene ($-\text{CH}_2$) group. The peaks at 1710 and 1654 cm^{-1} were related to the stretching vibrations of non-conjugate carbonyl and conjugate carbonate, respectively of carboxylic acid and ketone groups. The vibration of aromatic rings represented by the peaks at 1592, 1506, and 1420 cm^{-1} , indicates that the delignification occurred in *D. sinicus*. The intensity at 1461 cm^{-1} was attributed to the methoxyl C–H bending and C–C stretching in the aromatic skeleton. The absorption peaks at 1159, 1120 and 830 cm^{-1} represented the *p*-hydroxy phenylpropane (H), syringyl (S) and guaiacyl (G) units, respectively of

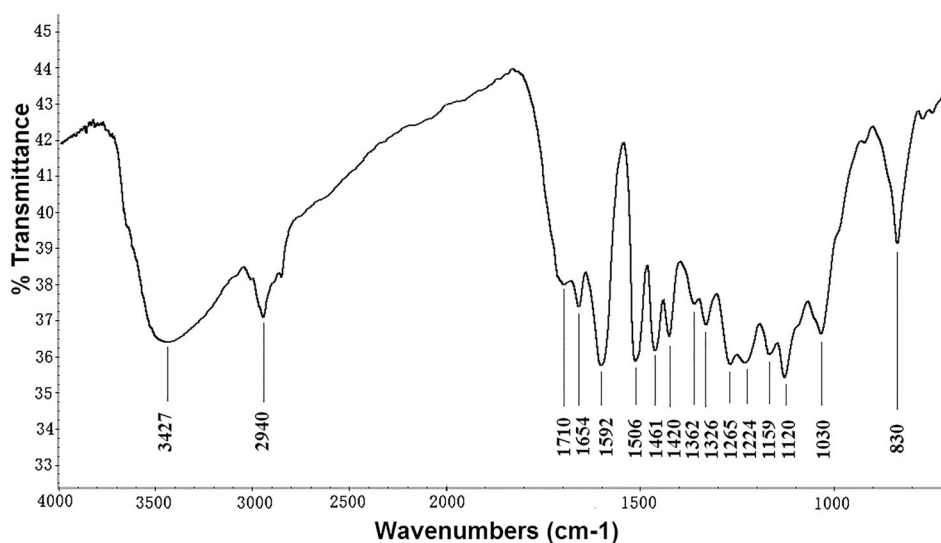


Figure 1. FT-IR spectrum of lignin fraction isolated from bamboo *D. sinicus*.

typical HGS-lignin. The bands at 1326 and 1265 cm^{-1} band were attributed to aromatic C–O stretching of S-units and/or condensed G- units at G_5 . The weak shoulder peak at 1362 cm^{-1} ascribed to the nonetherified phenolic -OH resulting from the cleavage at α -O-4' and β -O-4' linkage. The weak intensity of this peak demonstrating that the employed extraction method did not significantly cleave the linkage between α -O-4' and β -O-4' in the isolated lignin macromolecules. The peak at 1030 cm^{-1} was ascribed to the C–OH and C–O-

C stretching of the side groups and glycosidic bonds, respectively.

3.2. ^{13}C -NMR spectrum

The ^{13}C -NMR spectrum of the isolated MWL is shown in Figure 2. The peaks are in accordance with the earlier reported data (16–18). The signals between 104 and 168 ppm represent aromatic skeletons of the MWL. The syringyl (S) units are represented by peaks at 152.7 (C_3/C_5), 138.2

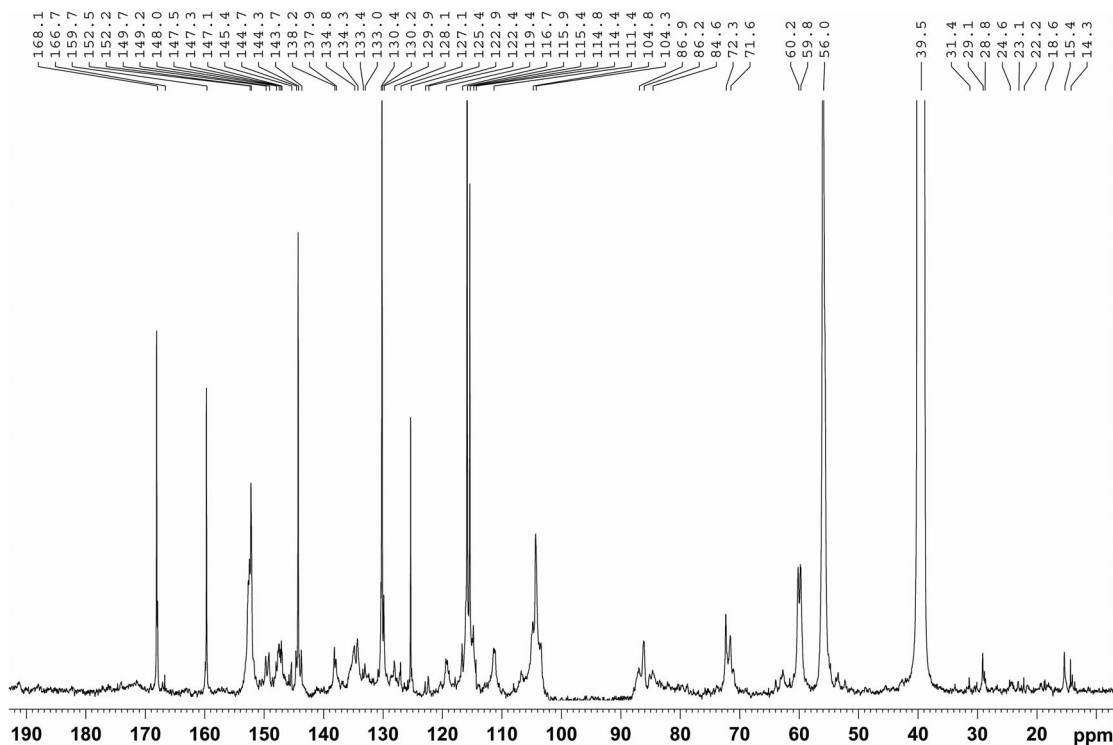


Figure 2. ^{13}C -NMR spectrum of milled wood lignin fraction isolated from bamboo *D. sinicus*.

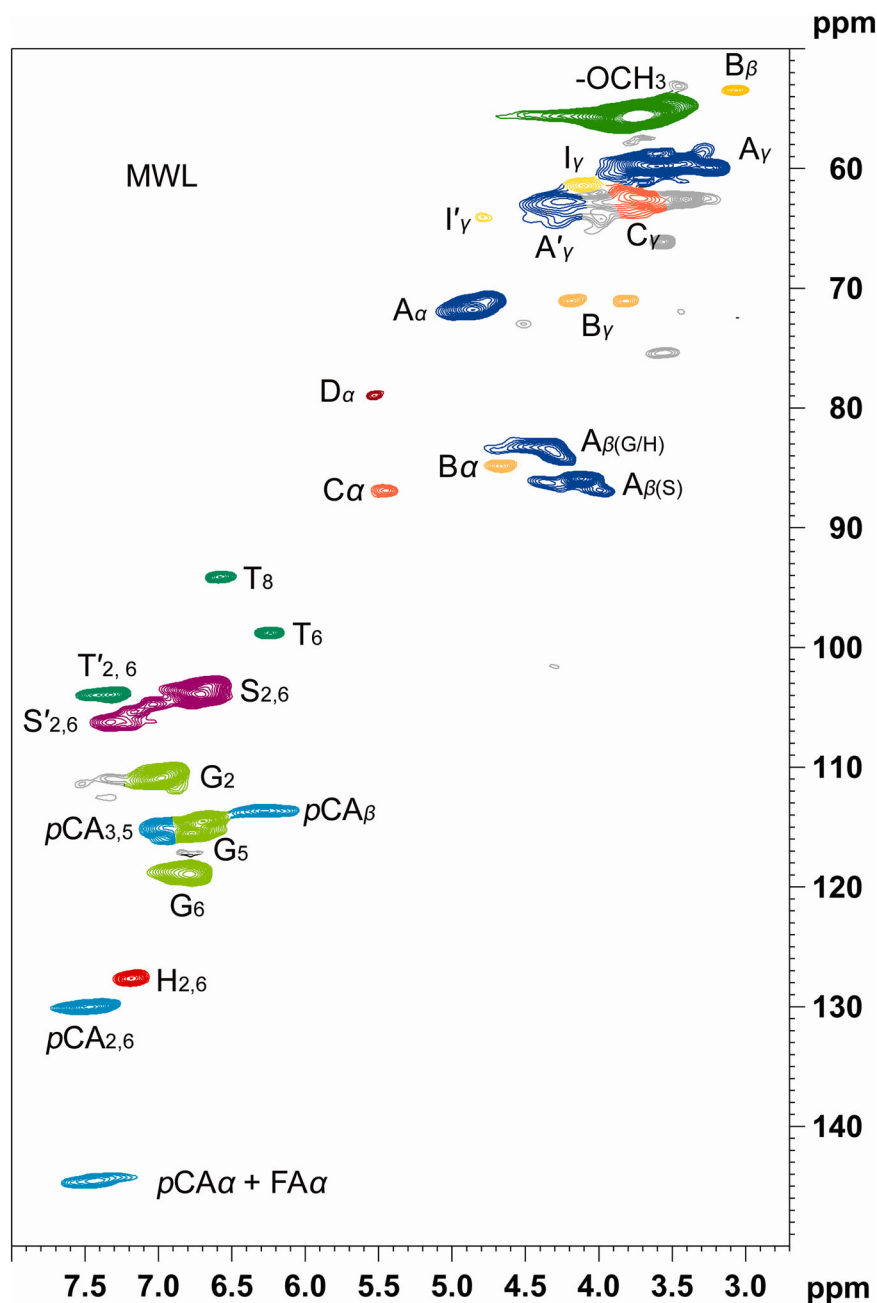


Figure 3. HSQC NMR spectrum of milled wood lignin fraction isolated from bamboo *D. sinicus*.

(C₄, etherified), 134.8 (C₁, etherified), 133.1 (C₁, etherified), 132.3 (C₁, non-etherified), 106.8 (C₂, C₆, with α -carbonyl) and 104.9 (C₂, C₆) ppm. The guaiacyl (G) units are indicated by the signals at 149.7 (C₃, etherified), 149.2 (C₃, etherified), 148.0 (C₄), 147.5 (C₄, non-etherified), 145.5, 134.3 (C₁, etherified), 133.1 (C₁, non-etherified), 119.4 (C₆), 114.8 (C₅), and 111.3 (C₂) ppm. The 129.9 (C₂, C₆) and 128.1 (C₂, C₆) ppm represented the *p*-hydroxyphenyl (H) units. This indicates that the isolated MWL is HGS-type lignin, which is consistent with FTIR results. Further, the presence of higher content was represented by the strong signals at 168.1 (C_γ), 159.8 (C₄), 144.3 (C_α), 130.1 (C₂/C₆), 125.3 (C₁), 116.7

(C₃/C₅) and 115.9 (C_β), which indicate that the alkaline condition did not cleave ester linkages between the *p*CA and MWL structural units.

One of the most important reactions for lignin degradation in alkaline media is the cleavage of β -O-4' structures. The distinguished signals at 72.3, 86.0, and 60.1 ppm corresponding to C- α , C- β , and C- γ , respectively of β -O-4' substructures, confirmed that the interlinkages are not cleaved significantly between the structural units of MWL under a neutral condition. Besides, the signals at 87.1, 71.4 and 62.7 indicated the existence of interunit C-C linkages such as C- α in β -5', C- γ in β - β' and C- γ with α -

carbonyl in β -5'/ β -O-4', respectively. The weak signals between 57 and 103 ppm represented the trace of hemicelluloses associated with MWL fractions.

3.3. 2D-HSQC NMR spectroscopy

The detailed chemical structures of the MWL isolated from *D. sinicus* were investigated by using 2D-HSQC NMR spectroscopy. The corresponding side chain region (δ_C/δ_H 50–90/2.5–5.6 ppm) and the aromatic region (δ_C/δ_H 100–155/6.0–8.5 ppm) are shown in Figure 3. The aliphatic region did not display significant information and was therefore ignored in this study. No obvious disparities were observed with the reported data (19–21). The side chain region of the spectrum

includes the interunit linkages such as β -O-4' aryl ethers substructures (A), β - β' / α -O- γ' / γ -O- α' resinol substructures (B), phenylcoumarans substructures (C) and spirodienone substructures (D). The prominent signals of methoxyl (-OCH₃) and β -O-4' aryl ethers indicating that they are dominant substructures of side chain region. The signals at δ_C/δ_H 72.3/4.83, δ_C/δ_H 72.3/4.83 and δ_C/δ_H 60.2/3.73 were attributed to the C $_{\alpha}$ -H $_{\alpha}$, C $_{\beta}$ -H $_{\beta}$ and C $_{\gamma}$ -H $_{\gamma}$ correlations of β -O-4' aryl ethers, respectively. C $_{\alpha}$ -H $_{\alpha}$, C $_{\beta}$ -H $_{\beta}$ and the double C $_{\gamma}$ -H $_{\gamma}$ correlations of the β - β' / α -O- γ' / γ -O- α' resinol substructures were represented by the signals at δ_C/δ_H 84.6/4.64, δ_C/δ_H 53.9/3.04 and δ_C/δ_H 71.6/3.83 & 4.16, respectively. The correlations appear at δ_C/δ_H 86.9/5.59 and 62.9/3.78 were associated with the C $_{\alpha}$ -H $_{\alpha}$ and C $_{\gamma}$ -H $_{\gamma}$ of phenylcoumaran

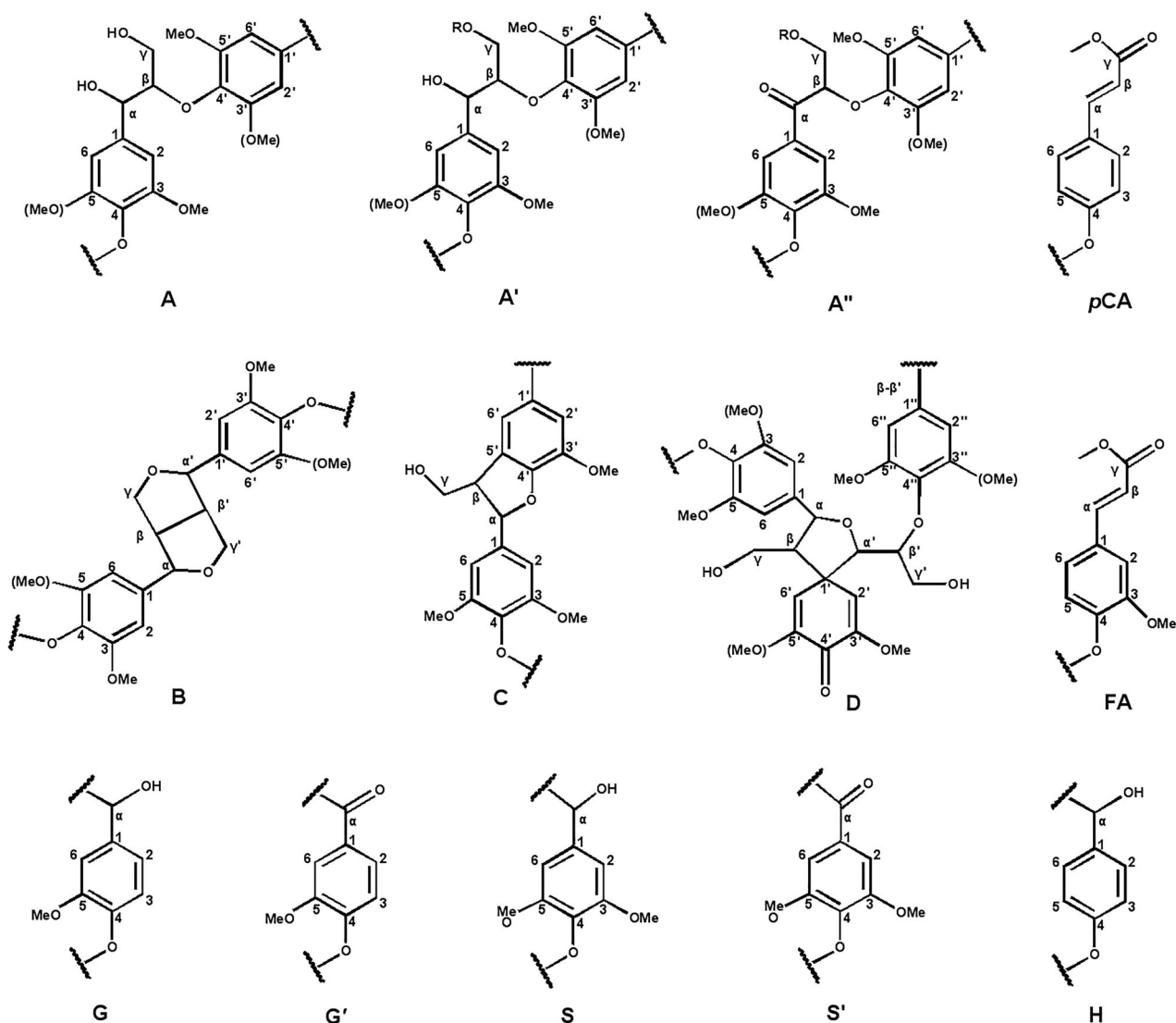


Figure 4. Main substructures presented in the isolated bamboo lignin fraction isolated from bamboo *D. sinicus*: (A) β -O-4' linkages; (A') γ -acetylated β -O-4' substructures; (A'') γ -p-coumaroylated β -O-4' linkages; (B) phenylcoumarane structures formed by β -5'/ α -O-4' linkages; (C) resinol structures formed by β - β' / α -O- γ' / γ -O- α' linkages; (D) spirodienone structures formed by β -1' linkages; (G) guaiacyl unit; (G') oxidized guaiacyl units with a Ca ketone; (S) syringyl unit; (S') oxidized syringyl unit linked a carbonyl group at Ca (phenolic); (FA) ferulate ester structures; (pCA) p-coumarate ester structures; (H) p-hydroxy phenylpropane unit.

Table 1. Quantitative characteristics of the ethanol dissolved bamboo lignin fraction by quantitative NMR method (per 100 Ar).

Linkage relative abundance (% of total side chains involved)	Relative proportion (%)
<i>Lignin inter-unit linkages</i>	
β -O-4' linked units (β -O-4', A/A)	79.5
Resinols (β - β' , B)	7.2
Phenylcoumarans (β -5', C)	5.6
Spirodienones (β -1', D)	4.0
<i>p</i> -Hydroxycinnamyl alcohols (F)	3.2
Percentage of γ -acetylation	1.1
<i>Lignin aromatic units</i>	
H (%)	9
S (%)	56
G (%)	35
S/G ratio	1.6

substructures (C), respectively. The weak signal at δ_C/δ_H 79.2/5.59 ppm corresponded to the C_α - H_α correlation of the spirodienone substructure.

The striking signal corresponding to the $C_{2,6}$ - $H_{2,6}$ correlation of S- unit in the δ_C/δ_H 104.3/6.68 aromatic region indicates the enrichment of S- units in isolated the MWL. The signals for G- units corresponding to their C_2 - H_2 , C_5 - H_5 , and C_6 - H_6 correlations were observed at δ_C/δ_H 111.4/6.95, δ_C/δ_H 114.8/6.71 and δ_C/δ_H 119.4/6.81, respectively. The signal for C_α oxidized S- units (carbonyl group, S') was observed at δ_C/δ_H 104.8/7.35. Apart from the S- and G- units, the signals corresponding to the esterified *p*-coumaric acid substructures (*p*CA) were appeared at in *p*CA were observed at δ_C/δ_H 128.1/7.16 (β -O-4'), δ_C/δ_H 130.2/7.51 ($C_{2,6}$ - $H_{2,6}$) and 116.7/6.32 ($C_{3,5}$ - $H_{3,5}$). In addition, the side chain cross-signals of *p*CA representing C_α and C_β were appeared at 144.3/7.51 and 115.4/

6.32 ppm, respectively. The $C_{2,6}$ - $H_{2,6}$ correlations of *p*-hydroxyphenyl units were observed at δ_C/δ_H 128.1/7.16. The molecular geometry of all the above-mentioned substructures of both side chain region and aromatic region are depicted in Figure 4.

3.4. 2D-HSQC NMR quantitative analysis

The relative content of the substructures in the isolated MWL of *D. sinicus* was calculated per 100 aromatic units (Ar) as reported elsewhere using equation (1) (22, 23) and listed in Table 1.

$$(X) = \frac{2D_{(X)}}{2D_{(90.0-78.0/6.0-2.5)}} * \frac{^{13}C_{(90.0-78.0)}}{^{13}C_{(163.0-103.6)}} * 600, \quad (1)$$

where $2_{(X)}$ is the resonance (volume) signal of the respective substructure (X), $2D_{(90.0-78.0/6.0-2.5)}$ is the total resonance of the corresponding cluster in the 2D spectrum, $^{13}C_{(90.0-78.0)}$ and $^{13}C_{(163.0-103.6)}$ are the resonance of the corresponding cluster in the ^{13}C spectrum and 600 is the number of aromatic carbons in 100 Ar. To quantify the amount of resinol, phenylcoumarane, and spirodienone substructures, the C_α - H_α correlations in the 2D spectrum were used, whereas for β -O-4' aryl ethers C_β - H_β correlations were selected for substructures used (24, 25).

In detail, β -O-4' aryl ether was the major inter-unit substructure present in isolated lignin fraction at the relative proportion of 79.5% per 100 aromatic units (Ar). In addition, β - β' resinol (R), β -5' phenylcoumaran, β -1' spirodienone, and *p*-hydroxycinnamyl alcohol substructures were existing in the relative proportion of

Table 2. A comparison on the amount of substructures in the MWL isolated from different species.

S. no	LCC	Relative composition (%)						S/G	Ref.
		β -O-4' aryl ether	Resinol	Phenylcoumaran	Spirodienones	<i>p</i> -hydroxycinnamyl alcohol			
1.	MWL (<i>Populus tomentosa</i> Carr.)	41.5	14.6	3.7	0.7	7.4	1.57	(24)	
2.	MWL (<i>Betula pendula</i>)	40.8	9.7	2.4	–	–	2.4	(22)	
3.	MWL (<i>Pinus taeda</i>)	27.4	4.4	9.8	–	–	–		
4.	MWL (<i>Quercus variabilis</i> Bl)	51.15	15.95	25.15	4.29	–	0.31	(30)	
5.	MWL- 2 yr (<i>E. grandis</i> \times <i>E. urophylla</i>)	49.5	14.5	2.6	1.2	–	1.99	(31)	
6.	MWL- 3 yr (<i>E. grandis</i> \times <i>E. urophylla</i>)	53.0	14.1	2.8	1.9	–	2.55		
7.	MWL- 4 yr (<i>E. grandis</i> \times <i>E. urophylla</i>)	55.2	14.7	2.3	0.8	–	2.43		
8.	MWL (<i>E. camaldulensis</i>)	45.2	12.0	2.7	Trace amount	–	1.5	(12)	
9.	MWL (<i>E. grandis</i>)	47.2	10.5	2.4	Trace amount	–	1.6		
10.	MWL (<i>E. urophydis</i>)	44.5	10.7	2.0	Trace amount	–	1.4		
11.	MWL (<i>D. sinicus</i>)	79.5	7.2	5.6	4.0	3.2	1.6	This work	

7.2%, 5.6%, 4.0%, and 3.2%, respectively. The percentage of acetylation at γ -carbon was found to be 1.1%.

It is also observed that the relative proportion of syringyl (S) unit (56%) was greater than that of the guaiacyl (G) unit (35%). The remaining 9% corresponds to the p-hydroxyl phenyl (H) unit. Theoretically, the S/G ratio is positively related to the content of β -O-4' substructures in lignin macromolecule (26). In the present study, the lignin isolated from bamboo (*D. sinicus*) shows a high S/G ratio of 1.6, which is in accordance with the results of dominant inter-unit linkages of β -O-4'. Comparison of the amount of the substructures in MWL isolated from different species (mentioned within the parenthesis) is shown in Table 2. The higher content of β -O-4' in MWL isolated from *D. sinicus* implies that most of the lignin is still remain in their MWL after extraction (27). The difference in the S/G ratio might due to the different morphological regions for each wood (7). The higher proportion of β -O-4' substructures is advantageous to the successive depolymerization and amelioration of lignin (28, 29). Thus the *D. sinicus* could serve as efficient feedstock for biorefinery industries (30, 31).

4. Conclusions

In summary, milled wood lignin (MWL) was isolated from the largest bamboo species, *D. sinicus*, under mild conditions. It was found that the MWL samples contain a high content of β -O-4' aryl ethers (~79.5% per 100 Ar) and syringyl units (S/G ~ 1.6), which will facilitate the successive depolymerization of aromatic chemicals in the MWL to energy. Besides, the techniques and findings described in this study enable the production of biochemicals and bioenergy from the lignin. As compared with the metals, carbon, polymers and ceramics (32–50), the lightweight makes this obtained lignin to be used together with other functional fillers for making multifunctional polymer nanocomposites suitable for various applications including electromagnetic interface (EMI) shielding (51–55), adsorbents for heavy metal, dye and spilled oil removal (56–64) and sensors (65–68), etc.

Acknowledgements

The authors are grateful for the financial support from the National Natural Science Foundation of China (31560195, 31760195), Education Department of Yunnan Province, China (2011Z040). Y. Meng appreciates the support from the Chinese Student Council scholarship.

Disclosure statement

No potential conflict of interest was reported by the authors.

Funding

This work was supported by Chinese Government Scholarship; National Natural Science Foundation of China [grant number 31560195, 31760195]; Education Department of Yunnan Province [grant number 2011Z040].

Notes on contributors

Zhengjun Shi, is currently an associate professor of chemical engineering at Key Laboratory for Forest Resources Conservation and Use in the Southwest Mountains of China, College of Chemical Engineering, Southwest Forestry University, China. His current research focuses on biomass chemistry, biomaterial, and bioenergy. E-mail: shizhengjun1979@163.com.

Gaofeng Xu is currently a lecturer of chemical engineering at College of Chemical Engineering, Southwest Forestry University, China. He is pursuing his doctoral degree in Chemical Processing Engineering of Forest Products. His research interests focus on biomass utilization for sustainable energy and environmental applications. E-mail: xgf0208@163.com.

Jia Deng is currently an associate professor of forestry at Key Laboratory for Forest Resources Conservation and Use in the Southwest Mountains of Ministry of Education, Southwest Forestry University, China. His current research focuses on biomass chemistry, biomaterial, and bioenergy. E-mail: dengjia1983@163.com.

Mengyao Dong is currently a joint Ph.D. student of Key Laboratory of Materials Processing and Mold (Zhengzhou University), Ministry of Education; National Engineering Research Center for Advanced Polymer Processing Technology, Zhengzhou University and Integrated Composites Laboratory (ICL) at University of Tennessee. His research interest focuses on multifunctional polymer nanocomposite coating.

Vignesh Murugadoss is a Ph.D. student of Centre for Nanoscience and Technology at Pondicherry University, Puducherry, undergoing Indo-US BASE internship at Integrated Composites Laboratory, Department of Chemical and Biomolecular Engineering at the University of Tennessee, Knoxville. His research interests focus on advanced functional materials for sustainable energy and environmental applications.

Chuntao Liu, is a full professor and director of the Key Laboratory of Materials Processing and Mold (Zhengzhou University), Ministry of Education; National Engineering Research Center for Advanced Polymer Processing Technology, Zhengzhou University. His current interests focus on the multifunctional polymer nanocomposites.

Qian Shao is a professor of the College of Chemical and Environmental Engineering, Shandong University of Science & Technology. Her research interest focuses on novel catalysts.

Dr. Shide Wu, is a Professor of Chemical Engineering, Zhengzhou University of Light Industry. His research interest focuses on the energy storage and conversion.

Dr. Zhanhu Guo, currently an Associate Professor of Chemical and Biomolecular Engineering at the University of Tennessee, obtained a Chemical Engineering Ph.D. degree from Louisiana State University (2005) and received three-year (2005–2008) post-doctoral training in Mechanical and Aerospace Engineering Department in University of California Los Angeles. Dr. Guo

directs the Integrated Composites Laboratory and chaired the Composite Division of American Institute of Chemical Engineers (AIChE, 2010–2011). His current research focuses on multifunctional nanocomposites for anti-corrosion, energy harvesting, electronic devices, environmental remediation, fire retardancy, and electromagnetic radiation shielding/absorption applications.

References

- [1] Mohanty, A.K.; Misra, M.; Hinrichsen, G. *Macromol. Mater. Eng.* **2000**, *276–277* (1), 1–24.
- [2] Dhillon, R.S.; von Wuehlisch, G. *Biomass Bioenergy* **2013**, *48*, 75–89.
- [3] Sheldon, R.A. *Green Chem.* **2014**, *16* (3), 950–963.
- [4] Ohrnberger, D., Introduction. In *The Bamboos of the World*, Ohrnberger, D., Ed. Elsevier: Amsterdam, **1999**; pp 1–6.
- [5] Feldman, D., Wood—chemistry, ultrastructure, reactions, by D. Fengel and G. Wegener, Walter de Gruyter, Berlin and New York, 1984, 613 pp. Price: 245 DM. *J. Polym. Sci., Polym. Lett. Ed.* **1985**, *23* (11), 601–602.
- [6] Yaku, F.; Tanaka, R.; Koshijima, T., In *Holzforchung*, **1981**; Vol. 35, p 177.
- [7] Guerra, A.; Filpponen, I.; Lucia, L.A.; Argyropoulos, D.S., *J. Agric. Food Chem.* **2006**, *54* (26), 9696–9705.
- [8] Shi, Z.-J.; Xiao, L.-P.; Deng, J.; Sun, R.-C., *BioEnergy Res.* **2013**, *6* (4), 1212–1222.
- [9] Xu, F.; Sun, R.-C.; Zhai, M.-Z.; Sun, J.-X.; Jiang, J.-X.; Zhao, G.-J., *J. Appl. Polym. Sci.* **2008**, *108* (2), 1158–1168.
- [10] Bjorkman, A., *Ind. Eng. Chem.* **1957**, *49* (9), 1395–1398.
- [11] Sluiter, A.; Ruiz, B.H.R.; Scarlata, C.; Sluiter, J.; Templeton, D.; Crocker, D. *Determination of Structural Carbohydrates and Lignin in Biomass*; National Renewable Energy Laboratory: USA, **2012**.
- [12] Wang, H.-M.; Wang, B.; Wen, J.-L.; Yuan, T.-Q.; Sun, R.-C. *ACS Sustainable Chem. Eng.* **2017**, *5* (12), 11618–11627.
- [13] Shi, Z.; Jia-Deng, L.-P.X.; Xu, F.; Sun, R. *J. Appl. Polym. Sci.* **2012**, *125* (4), 3290–3301.
- [14] Scalbert, A.; Monties, B.; Guittet, E.; Lallemand, J.Y. *Holzforchung*, **1986**; Vol. 40, p 119.
- [15] Xu, F.; Sun, R.-C.; Sun, J.-X.; Liu, C.-F.; He, B.-H.; Fan, J.-S., *Anal. Chim. Acta* **2005**, *552* (1), 207–217.
- [16] Xiao, L.-P.; Shi, Z.-J.; Xu, F.; Sun, R.-C.; Amar, K.M., *Spectrosc. Spectral Anal.* **2011**, *31* (9), 2369–2376.
- [17] Kang, S.; Xiao, L.; Meng, L.; Zhang, X.; Sun, R. *Int. J. Mol. Sci.* **2012**, *13* (11), 15209–15226.
- [18] Sun, S.-L.; Wen, J.-L.; Ma, M.-G.; Sun, R.-C.; Jones, G.L., *Ind. Crops Prod.* **2014**, *56*, 128–136.
- [19] Xiao, L.-P.; Shi, Z.-J.; Xu, F.; Sun, R.-C., In *Holzforchung*, **2012**; Vol. 66, p 295.
- [20] del Río, J.C.; Prinsen, P.; Rencoret, J.; Nieto, L.; Jiménez-Barbero, J.; Ralph, J.; Martínez, Á.T.; Gutiérrez, A., *J. Agric. Food Chem.* **2012**, *60* (14), 3619–3634.
- [21] Samuel, R.; Foston, M.; Jiang, N.; Allison, L.; Ragauskas, A.J., *Polym. Degrad. Stab.* **2011**, *96* (11), 2002–2009.
- [22] Balakshin, M.; Capanema, E.; Gracz, H.; Chang, H.-M.; Jameel, H., *Planta* **2011**, *233* (6), 1097–1110.
- [23] Tarasov, D.; Leitch, M.; Fatehi, P., *Biotechnol. Biofuels* **2018**, *11* (1), 269.
- [24] Yuan, T.-Q.; Sun, S.-N.; Xu, F.; Sun, R.-C., *J. Agric. Food Chem.* **2011**, *59* (19), 10604–10614.
- [25] Zhang, L.; Gellerstedt, G., *Magn. Reson. Chem.* **2007**, *45* (1), 37–45.
- [26] Wen, J.-L.; Xue, B.-L.; Xu, F.; Sun, R.-C.; Pinkert, A., *Ind. Crops Prod.* **2013**, *42*, 332–343.
- [27] Chen, T.-Y.; Wang, B.; Shen, X.-J.; Li, H.-Y.; Wu, Y.-Y.; Wen, J.-L.; Liu, Q.-Y.; Sun, R.-C., *RSC Adv.* **2017**, *7* (6), 3376–3387.
- [28] Lu, H.; Zhang, L.; Liu, C.; He, Z.; Zhou, X.; Ni, Y., *Cellulose* **2018**, *25* (12), 7043–7051.
- [29] Xu, G.; Shi, Z.; Zhao, Y.; Deng, J.; Dong, M.; Liu, C.; Murugadoss, V.; Mai, X.; Guo, Z., *Int. J. Biol. Macromol.* **2019**, *126*, 376–384.
- [30] Yang, L.; Wang, D.; Zhou, D.; Zhang, Y.; Yang, T., *Int. J. Biol. Macromol.* **2017**, *97*, 164–172.
- [31] Zhao, B.-C.; Chen, B.-Y.; Yang, S.; Yuan, T.-Q.; Charlton, A.; Sun, R.-C., *ACS Sustainable Chem. Eng.* **2017**, *5* (1), 1113–1122.
- [32] Qu, Z.; Shi, M.; Wu, H.; Liu, Y.; Jiang, J.; Yan, C. *J. Power Sources.* **2019**, *410–411*, 179–187.
- [33] Lin, Z.; Lin, B.; Wang, Z.; Chen, S.; Wang, C.; Dong, M.; Gao, Q.; Shao, Q.; Wu, S.; Ding, T. *Chemcatchem.* **2019**, *11*, 2217–2222.
- [34] Yang, J.; Yang, W.; Wang, X.; Dong, M.; Liu, H.; Wujcik, E. K.; Shao, Q.; Ding, T.; Guo, Z. *Macromol. Chem. Phys.* **2019**. doi:10.1002/macp.201800567. in press.
- [35] Xu, G.; Shi, Z.; Zhao, Y.; Deng, J.; Dong, M.; Liu, C.; Murugadoss, V.; Mai, X.; Guo, Z. *Int. J. Biol. Macromol.* **2019**, *126*, 376–384.
- [36] Zhao, Z.; Guan, R.; Zhang, J.; Zhao, Z.; Bai, P. *Acta Metall. Sin. (Engl. Lett.)* **2017**, *30*, 66–72.
- [37] Zhao, Z.; Bai, P.; Guan, R.; Murugadoss, V.; Liu, H.; Wang, X.; Guo, Z. *Mater. Sci. Eng. A.* **2018**, *734*, 200–209.
- [38] Zhao, Y.; Qi, L.; Jin, Y.; Wang, K.; Tian, J.; Han, P. *J. Alloys Compounds*, **2015**, *647*, 1104–1110.
- [39] Zhao, Y.; Zhang, B.; Hou, H.; Chen, W.; Wang, M. *J. Mater. Sci. Technol.* **2019**, *35*, 1044–1052.
- [40] Zhao, Y.; Zhang, B.; Yuan, Y.; Guo, Q.; Hou, H. *J. Solid State Chem.* **2019**, *276*, 232–237.
- [41] Zhao, Y.; Tian, X.; Zhao, B.; Sun, Y.; Guo, H.; Dong, M.; Liu, H.; Wang, X.; Guo, Z.; Umar, A.; Hou, H. *Sci. Adv. Mater.* **2018**, *10*, 1793–1804.
- [42] Shi, Z.; Jia, C.; Wang, D.; Deng, J.; Xu, G.; Wu, C.; Dong, M.; Guo, Z. *Int. J. Biol. Macromol.* **2019**, *133*, 964–970.
- [43] Zhu, G.; Cui, X.; Zhang, Y.; Chen, S.; Dong, M.; Liu, H.; Shao, Q.; Ding, T.; Wu, S.; Guo, Z. *Polymer.* **2019**, *172*, 415–422.
- [44] Berndt, A.; Hwang, J.; Islam, A.; Urbas, A. M.; Ku, Z.; Lee, S.; Czapleski, D.; Dong, M.; Shao, Q.; Wu, S.; et al. *Polymer.* **2019**, *176*, 118–126.
- [45] Jiang, D.; Murugadoss, V.; Wang, Y.; Lin, J.; Ding, T.; Wang, Z.; Shao, Q.; Wang, C.; Liu, H.; Lu, N. *Polym. Rev.* **2019**, *59*, 280–337.
- [46] Du, W.; Wang, X.; Zhan, J.; Sun, X.; Kang, L.; Jiang, F.; Zhang, X.; Shao, Q.; Dong, M.; Liu, H.; Murugadoss, V.; Guo, Z. *Electrochim. Acta* **2019**, *296*, 907–915.
- [47] Dong, M.; Li, Q.; Liu, H.; Liu, C.; Wujcik, E.; Shao, Q.; Ding, T.; Mai, X.; Shen, C.; Guo, Z. *Polymer* **2018**, *158*, 381–390.
- [48] Idrees, M.; Batool, S.; Kong, J.; Zhuang, Q.; Liu, H.; Shao, Q.; Lu, N.; Feng, Y.; Wujcik, E.K.; Gao, Q.; Ding, T.; Wei, R.; Guo, Z. *Electrochim. Acta* **2019**, *296*, 925–937.
- [49] Sun, H.; Yang, Z.; Pu, Y.; Dou, W.; Wang, C.; Wang, W.; Hao, X.; Chen, S.; Shao, Q.; Dong, M.; et al. *J. Colloid Interf. Sci.* **2019**, *547*, 40–49.
- [50] Zhao, Z.; An, H.; Lin, J.; Feng, M.; Murugadoss, V.; Ding, T.; Liu, H.; Shao, Q.; Man, X.; Wang, N. *Chem. Rec.* **2019**, *19*, 873–882.

- [51] Wang, Z.; Wei, R.; Gu, J.; Liu, H.; Liu, C.; Luo, C.; Kong, J.; Shao, Q.; Wang, N.; Guo, Z. *Carbon*. **2018**, *139*, 1126–1135.
- [52] Wang, C.; Murugadoss, V.; Kong, J.; He, Z.; Mai, X.; Shao, Q.; Chen, Y.; Guo, L.; Liu, C.; Angaiah, S. *Carbon*. **2018**, *140*, 696–733.
- [53] Wang, L.; Qiu, H.; Liang, C.; Song, P.; Han, Y.; Han, Y.; Gu, J.; Kong, J.; Pan, D.; Guo, Z. *Carbon*. **2019**, *141*, 506–514.
- [54] Gu, H.; Zhang, H.; Ma, C.; Xu, X.; Wang, Y.; Wang, Z.; Wei, R.; Liu, H.; Liu, C.; Shao, Q. *Carbon*. **2019**, *142*, 131–140.
- [55] Wu, N.; Liu, C.; Xu, D.; Liu, J.; Liu, W.; Shao, Q.; Guo, Z. *ACS Sustain. Chem. Eng.*, **2018**, *6*, 12471–12480.
- [56] Wu, N.; Liu, C.; Xu, D.; Liu, J.; Liu, W.; Liu, H.; Zhang, J.; Xie, W.; Guo, Z. *J. Mater. Chem. C*. **2019**, *7*, 1659–1669.
- [57] Qian, Y.; Yuan, Y.; Wang, H.; Liu, H.; Zhang, J.; Shi, S.; Guo, Z.; Wang, N. *J. Mater. Chem. A* **2018**, *6*, 24676–24685.
- [58] Xie, P.; He, B.; Dang, F.; Lin, J.; Fan, R.; Hou, C.; Liu, H.; Zhang, J.; Ma, Y.; Guo, Z. *J. Mater. Chem. C* **2018**, *6*, 8812–8822.
- [59] Li, Z.; Wang, B.; Qin, X.; Wang, Y.; Liu, C.; Shao, Q.; Wang, N.; Zhang, J.; Wang, Z.; Shen, C.; Guo, Z. *ACS Sustain. Chem. Eng.* **2018**, *6*, 13747–13755.
- [60] Gong, K.; Hu, Q.; Yao, L.; Li, M.; Sun, D.; Shao, Q.; Qiu, B.; Guo, Z. *ACS Sustain. Chem. Eng.* **2018**, *6*, 7283–7291.
- [61] Wang, Y.; Zhou, P.; Luo, S.; Liao, X.; Wang, B.; Shao, Q.; Guo, X.; Guo, Z. *Langmuir* **2018**, *34*, 7859–7868.
- [62] Ma, Y.; Lyu, L.; Guo, Y.; Fu, Y.; Shao, Q.; Wu, T.; Guo, S.; Sun, K.; Guo, X.; Wujcik, E.K.; Guo, Z. *Polymer* **2017**, *128*, 12–23.
- [63] Huang, J.; Cao, Y.; Shao, Q.; Peng, X.; Guo, Z. *Ind. Eng. Chem. Res.* **2017**, *56*, 10689–10701.
- [64] Zhang, X.; Wang, X.; Liu, X.; Lv, J.; Wang, Y.; Zheng, G.; Liu, H.; Liu, C.; Guo, Z.; Shen, C. *ACS Sustain. Chem. Eng* **2018**, *6*, 12580–12585.
- [65] Lu, Y.; Biswas, M.C.; Guo, Z.; Jeon, J.; Wujcik, E.K. *Biosensors Bioelectronics* **2019**, *123*, 167–177.
- [66] Gu, H.; Xu, X.; Dong, M.; Xie, P.; Shao, Q.; Fan, R.; Liu, C.; Wu, S.; Liu, W.; Liu, J.; et al. *Carbon*. **2019**, *147*, 550–558.
- [67] Liu, H.; Li, Q.; Zhang, S.; Yin, R.; Liu, X.; He, Y.; Dai, K.; Shan, C.; Guo, J.; Liu, C.; Shen, C.; Wang, X.; Wang, N.; Wang, Z.; Wei, R.; Guo, Z. *J. Mater. Chem. C* **2018**, *6*, 12121–12141.
- [68] Wei, H.; Wang, H.; Xia, Y.; Cui, D.; Shi, Y.; Dong, M.; Liu, C.; Ding, T.; Zhang, J.; Ma, Y.; Wang, N.; Wang, Z.; Sun, Y.; Wei, R.; Guo, Z. *J. Mater. Chem. C* **2018**, *6*, 12446–12467.